Nonoverlap of the Star Unfolding*

Boris Aronov† and Joseph O'Rourke‡

Abstract

The star unfolding of a convex polytope with respect to a point x is obtained by cutting the surface along the shortest paths from x to every vertex, and flattening the surface on the plane. We establish two main properties of the star unfolding: (1) It does not self-overlap: its boundary is a simple polygon. (2) The ridge tree in the unfolding, which is the locus of points with more than one shortest path from x, is precisely the Voronoi diagram of the images of x, restricted to the unfolding.

These two properties permit the conceptual simplification of several algorithms concerned with shortest paths on polytopes, and sometimes a worst-case complexity improvement as well: for constructing the ridge tree, for finding the exact set of all shortest-path "edge sequences," and for computing the geodesic diameter of a polytope.

Our results suggest conjectures on "unfoldings" of general convex surfaces.

---

*Part of the research for this paper was carried out while the first author was at the DIMACS Center, Rutgers University. The second author's research was supported by NSF grant CCR-882194.

†Computer Science Department, Polytechnic University, Brooklyn, NY 11201 USA

‡Department of Computer Science, Smith College, Northampton, MA 01063 USA

1 Introduction

A new way of organizing the set of all shortest paths from a fixed point x on the surface $\mathcal{P}$ of a (convex) polytope was introduced by Agarwal et al in [AAOS90] and by Chen and Han in [CH90], independently and simultaneously. The main idea already appears in Aleksandrov's work forty years ago, although he uses it only to show that $\mathcal{P}$ can be triangulated.[1] We will follow [AAOS90] and refer to this structure as the ***star unfolding*** of a polytope, so called because of the "star-like" appearance of the planar unfolding of the paths.[2] The star unfolding may be obtained by cutting the polytope along the shortest paths from x to each vertex of $\mathcal{P}$, and flattening the surface on the plane. The star unfolding contrasts with the ***source unfolding*** [SS86], which simply lays out all shortest paths around the source x. In comparison, the star unfolding arranges the paths around their destinations, the ends opposite x. These notions will be made precise in Section 1.1.

The star unfolding has proven to be a useful structure for algorithms that involve shortest paths, as detailed in [AAOS90] and [CH90]. However, an unfortunate complication was left unresolved in both of these papers: it was not known whether the star unfolding might overlap in a planar layout. This uncertainty forced the algorithms to be unpleasantly complex. The first result of this paper is that indeed the star unfolding does not overlap (Theorem 9.1).

The second result is that the "ridge tree," the locus of points with more than one shortest path from the source, is precisely the Voronoi diagram of the source images in the star unfold-

---

[1] See [Ale58, p. 171] and [Ale55, p. 226].

[2] The star unfolding is not necessarily a star-shaped polygon!

ing, restricted to the unfolding (Theorem 10.2). This relationship was suspected by researchers, but never established. An illustration is shown in Fig. 1.

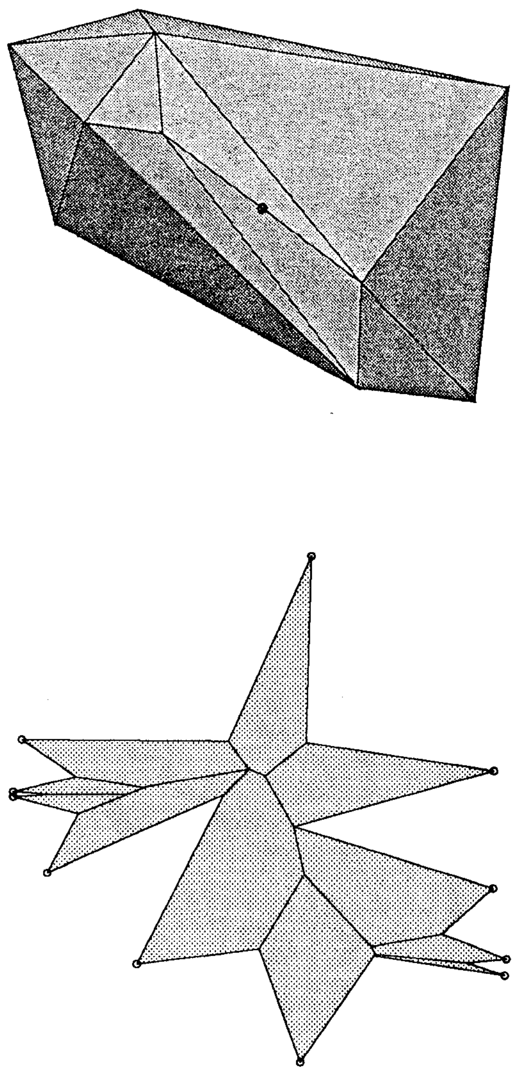

Figure 1: (a) A polytope of 11 corners; x is marked. (b) The star unfolding with respect to x, with the ridge tree shown.

Together these results both conceptually simplify previous algorithms, and in several instances improve the worst-case time complexity as well. In particular, algorithms for constructing the ridge tree, for finding shortest-path edge sequences, and for computing the diameter of a polytope are all improved. These consequences are discussed briefly in Section 12; details will appear in [AAOS91].

1.1 Definitions and Basic Properties

In this section we give formal definitions of the star unfolding and the ridge tree, taken largely from [AAOS90]. Consider the surface $\mathcal{P}$ of a convex polytope in $\mathbb{R}^3$ with n vertices. We reserve the term *corners* to refer to vertices of $\mathcal{P}$.

1.1.1 Ridge Trees

Given a point x on $\mathcal{P}$, $y \in \mathcal{P}$ is a *ridge point* with respect to x if there are two or more distinct shortest paths between x and y. Ridge points with respect to x form a *ridge tree* T_x embedded on $\mathcal{P}$,[3] whose leaves are corners of $\mathcal{P}$, and whose internal vertices have degree at least three and correspond to points of $\mathcal{P}$ with three or more distinct shortest paths to x. To simplify our discussion we assume that x does not lie at a corner and has a unique shortest path to each corner. We define a *ridge* as a maximal connected subset of T_x consisting of points with exactly two distinct shortest paths to x, and containing no corners of $\mathcal{P}$. These are the "edges" of T_x. Ridges are (open) shortest paths [AAOS90]. A *ridge vertex* is a point of the ridge tree shared by more than one ridge. Additionally we consider each corner a ridge vertex. Under the above assumptions on x each corner has exactly one incident ridge.

Let a *ridge point* be a point of $\mathcal{P}$ that lies on the ridge tree of some vertex. We will often restrict the source of shortest paths to be a non-ridge point.

1.1.2 Star Unfolding

Let $x \in \mathcal{P}$ be a non-corner, non-ridge point, so that there is a unique shortest path connecting x to each corner of $\mathcal{P}$. These paths are called *cuts* and are comprised of *cut points*. The cuts together with edges of $\mathcal{P}$ induce a convex decomposition of $\mathcal{P}$, which we will treat as a surface $\mathcal{P}_x$ of a polytope. It is geometrically identical to $\mathcal{P}$, but combinatorially different.

Now form a two-dimensional complex from the faces of $\mathcal{P}_x$ as follows. The cells of the com-

[3] For smooth surfaces (Riemannian manifolds), the ridge tree is known as the "cut locus" [Kob67].

plex are the faces of $\mathcal{P}_x$, each a compact convex polygon. For each pair of adjacent faces of $\mathcal{P}_x$ sharing an edge of $\mathcal{P}_x$, which is a portion of an edge of $\mathcal{P}$, topologically identify the two faces along that edge. We define the *star unfolding* S_x as the resulting two-dimensional complex.[4] We assume that the complex carries with it labeling information consistent with $\mathcal{P}_x$. Its polygonal boundary ∂S_x consists entirely of edges originating from cuts. It is shown in [AAOS90] that S_x is topologically equivalent to a closed disk.

We think of S_x as laid out in the plane with adjacent faces placed on opposite sides of the line containing their shared edge. The essence of Theorem 9.1 is that non-adjacent faces in such a layout do not overlap either.

1.1.3 Image Map

For $p \in \mathcal{P}$, let $Im(p)$ be the set of points in S_x to which p maps. Thus $Im(p)$ for a point p not on a cut is a single point, $Im(x)$ is a set of n distinct points in S_x, a non-corner point $y \in \mathcal{P}$ distinct from x and lying on a cut has exactly two images in S_x, and the corners of $\mathcal{P}$ map to single points. A "segment" in S_x is a connected object that maps to a line segment when S_x is unfolded in the plain. More formally, a curve $s \subset S_x$ is a *segment* in S_x if its preimage $Im^{-1}(s)$ is a geodesic on $\mathcal{P}$. In particular, ∂S_x is a cycle of $2n$ segments. In addition, for a point $y \in \mathcal{P}$, any shortest path π from x to y maps to a segment $\pi^* \subset S_x$ connecting an element of $Im(y)$ to an element of $Im(x)$ [AAOS90].

In [AAOS90] care was taken to distinguish objects on $\mathcal{P}$ and in S_x. Here we will be intentionally less careful, to take advantage of the notational simplification gained from the natural correspondence between a set $Q \subseteq \mathcal{P}$ and $Im(Q) \subseteq S_x$: unless confusion is possible, we will call both Q.

1.1.4 Source Images

Let $X = Im(x) = \{x_1, x_2, ..., x_n\}$, the source images in a planar layout of S_x. We label the source images and the corners so that they appear as $p_1 x_1 p_2 x_2 ... x_{i-1} p_i x_i p_{i+1} x_{i+1} ... p_n x_1$ in counterclockwise order around S_x.

[4]We will not distinguish the complex from the natural intrinsic metric space defined on the complex.

1.1.5 Peels

Let a *peel* be the closure of a connected component of the set obtained by removing from $\mathcal{P}$ both the ridge tree T_x and the cuts. A peel is isometric to a convex polygon [SS86]. Each peel's boundary consists of x, the shortest paths to two consecutive corners of $\mathcal{P}$, p_i and p_{i+1}, and the unique path in T_x connecting p_i to p_{i+1}. A peel can be thought of as the collection of all the shortest paths emanating from x "between" $\pi(x, p_i)$ and $\pi(x, p_{i+1})$.

1.2 Key Ideas

Both main theorems are proved by induction on the number of corners. There are three key ideas to their proofs.

First, the reduction from n to $n-1$ corners is chosen to occur in a particular part of the ridge tree, a spot that is shown to always exist.

Second, a powerful theorem of Aleksandrov is used to show that the reduction indeed results in a polytope, to which the induction hypothesis then applies.

Finally, the induction hypotheses are stronger than the bare statements of nonoverlap and the indicated Voronoi property: for both theorems we prove additional structural properties of the unfolding to establish the results.

1.3 Outline

The next section establishes a lemma about ridge trees that identifies the area where the reduction is made. Section 3 then details the reduction. Section 4 describes Aleksandrov's theorem, and Section 5 works out the consequences for the star unfolding. The basis of the induction proofs is explored in Section 6. Key geometric properties of the reduction are established in Section 7. All the material up to this point is used in common for the two main theorems.

Section 8 introduces structural constraints on the star unfolding, and in Section 9 the nonoverlap theorem is proved. The proof of the Voronoi property is given in Section 10.

Extensions to smooth surfaces and algorithmic consequences are discussed briefly in Sections 11 and 12 respectively.[5]

[5]This paper is a 3:1 reduction of [AO91]. All omitted proofs may be found in the full version.

2 Tree Lemmas

This section establishes a simple property of ridge trees (Lemma 2.2), which will be used to identify the location on the polytope where the reduction will be effected. The notion of "curvature" will be used throughout the paper. The *curvature* at a corner p of $\mathcal{P}$ is 2π minus the sum of the face angles incident to p. The curvature of every corner is strictly between 0 and 2π. We will use α_i to represent the curvature at p_i. All curvature on a polytope is concentrated at the corners.

Lemma 2.1 (Gauss) *The sum of the curvatures of all vertices of $\mathcal{P}$ is 4π.*

Lemma 2.2 *Any ridge tree T_x contains a ridge vertex adjacent to two consecutive corners of $\mathcal{P}$, whose sum of curvatures is no more than 2π. For a polytope with $n > 4$ vertices, the sum is strictly less than 2π; for $n = 4$, the curvatures might sum to exactly 2π.*

□

The fact that the sum can be exactly 2π when $n = 4$ will necessitate special arguments in the base cases of the induction proofs of the two main theorems.

3 Reduction

Let v be the ridge vertex adjacent to the two consecutive corners p_i and p_{i+1}, guaranteed by Lemma 2.2 to have curvatures totaling at most 2π. Make a planar layout of the portion of S_x containing the peels for x_{i-1}, x_i, and x_{i+1}. These three peels meet at v, and do not overlap, because each peel is convex and occupies a disjoint angular wedge emanating from v. The reduction that permits us to use the induction hypothesis replaces the two corners p_i and p_{i+1} of $\mathcal{P}$ with a new corner p'; eventually we will show this produces a new polytope of $n-1$ corners $\mathcal{P}'$. We now describe the reduction.

We define $R \subset S_x$ to be the simple polygon $(v, x_{i-1}, p_i, x_i, p_{i+1}, x_{i+1})$, a hexagon that is contained in the union of the three peels discussed above. This region is shaded in Fig. 2. R will denote the corresponding region on $\mathcal{P}$ as well. We excise R from the complex S_x, and replace it with a region R', which is the planar quadrilateral $(v, x_{i-1}, p', x_{i+1})$. Let $\angle abc$ denote the angle at b contained counterclockwise between the rays ba and bc. The corner point p' is placed on the bisector of $\angle x_{i-1} v x_{i+1}$ so that its external angle (i.e., its curvature) is the sum of the curvatures at p_i and p_{i+1}: $\alpha' = \alpha_i + \alpha_{i+1}$. Again see Fig. 2.

Lemma 3.1 *For $n > 4$, there is a point p' on the ray bisecting $\angle x_{i-1} v x_{i+1}$, whose external angle is $\alpha_i + \alpha_{i+1}$. For $n = 4$, the same holds unless $\alpha_i + \alpha_{i+1} = 2\pi$.*

□

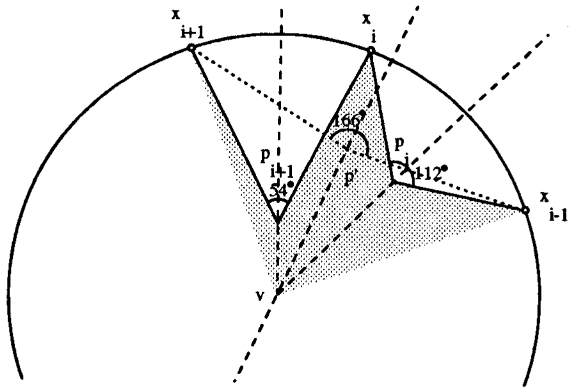

Figure 2: The reduction, shown with R and R' superimposed.

This lemma demonstrates that the region R' is well-defined. Replacing R by R' produces a new complex $S'_x = (S_x - R) \cup R'$, which has $n-1$ "corners." The key to the success of the induction proof is to show that this complex corresponds to a (unique) polytope $\mathcal{P}'$. This is by no means obvious, but fortunately it is a corollary of a beautiful theorem of Aleksandrov, which we describe in the next section.

4 Aleksandrov's Theorem

Definition 4.1 *A* net ([Ale58, p. 44]) *is a complex of polygons with edges topologically identified, such that*

1. *Identified edges have the same length.*
2. *There is a path from every polygon to every other.*
3. *Every edge of a polygon is identified with at most one edge of another polygon.*

Theorem 4.2 (Aleksandrov) *"Every net that is homeomorphic to a sphere and whose* *angle sum at every vertex is $\leq 2\pi$, corresponds to a closed convex polyhedron."* [Ale58, p. 169].

The star unfolding S_x, with the identification of the two images of cuts from x to each corner, is a net homeomorphic to a sphere, obviously corresponding to the polytope $\mathcal{P}$ from which it is derived.

Lemma 4.3 *Aleksandrov's theorem applies to S'_x.*

□

5 Reduced Star Unfolding

By Lemma 4.3 and Theorem 4.2, S'_x folds to a polytope $\mathcal{P}'$, to which the induction hypothesis applies. Now we concentrate on the transformation from $\mathcal{P}'$ to $\mathcal{P}$ as represented in Fig. 3: the region R' is cut out and replaced by R, the reverse of the reduction discussed in Section 3. The goal of this section is to show that S'_x is

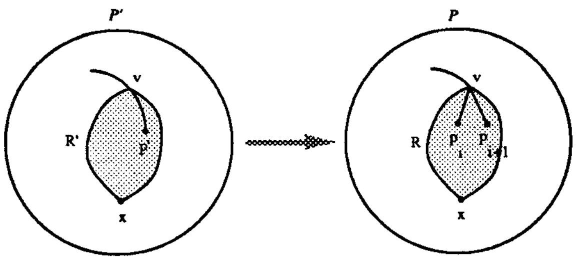

Figure 3: The reduction reversed, viewed on the polytope surface.

precisely the star unfolding of $\mathcal{P}'$. Namely, the star unfolding of $\mathcal{P}'$ is exactly the same as S_x, the unfolding of $\mathcal{P}$, except for the regions R and R' cut and pasted. This will permit us to reason entirely with the unfoldings.

Lemma 5.1 *S'_x is the star unfolding of $\mathcal{P}'$.*

□

Corollary 5.2 *The ridge trees are the same in S_x and S'_x outside the regions that differ between these two unfoldings: $T'_x - R' = T_x - R$*

□

Corollary 5.3 *In $\mathcal{P}'$, x is not a ridge point of any corner of S'_x.*

□

This permits us to assume "non-ridgeness" inductively.

5.1 More Notation

Lemma 5.1 permits the following view of the reduction, which we will adopt in the remainder of the paper. S_x and S'_x differ only in the replacement of two corners and one source image in S_x, by one corner in S'_x. If we lay S_x and S'_x on top of one another in the plane, the $n-1$ source images that they share will coincide. We will therefore use the same labels for these sources

$$x_1, x_2, \ldots, x_{i-1}, x_{i+1}, \ldots, x_n$$

and for the common corners.

$$p_1, p_2, \ldots, p_{i-1}, p_{i+2}, \ldots, p_n.$$

In what follows x_i will always refer to the source image of S_x removed by the reduction, and p_i and p_{i+1} will refer to the two corners removed; p' will be used to denote the corner added to S'_x. In general, primes will denote quantities of S'_x.

5.2 Example

Fig. 4(a) shows an unfolding of a square pyramid, with x at the midpoint of one of the base square's edges. Fig. 4(b) shows the star unfolding, and a region R identified for the reduction step of the induction. Fig. 4(c) shows the unfolding after R is replaced by R'. If Fig. 4(d), which is Fig. 4(c) redrawn, is folded along the lines shown, the result is a convex polyhedron (a tetrahedron), as guaranteed by Aleksandrov's theorem. If the reduction is applied to Fig. 4(d), the base case of the induction is reached, a doubly-covered triangle. All three star unfoldings produced in this reduction process are shown in Fig. 5.

6 Induction Basis

6.1 Generic case: Doubly-covered triangle ($n = 3$)

Each reduction step reduces n, the number of vertices, by 1. The "generic" basis of the induction is $n = 3$, when the star unfolding is a hexagon: three corners and three source images. An example is shown in Fig. 5. The corresponding polytope is a flat, "doubly-covered" triangle with x on one side, a degenerate case permitted by Aleksandrov's theorem.

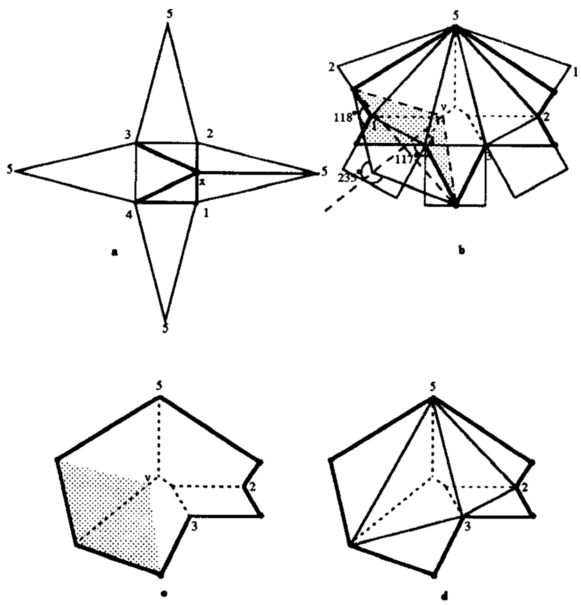

Figure 4: The star unfolding of a pyramid reduced to a tetrahedron.

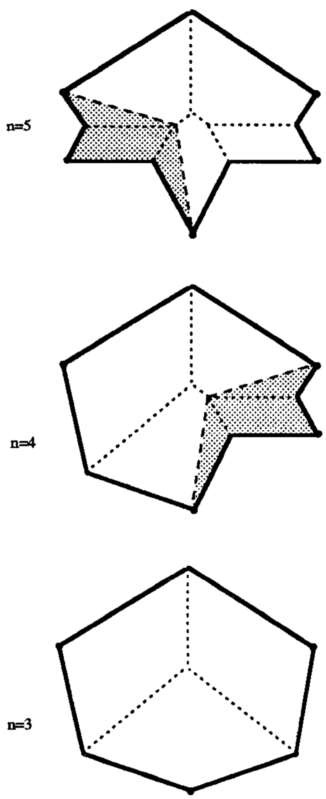

Figure 5: Three star unfoldings from the pyramid.

Although this doubly-covered triangle has zero volume, it behaves as the surface of any other convex polytope.

6.2 Special case: Special tetrahedron ($n = 4$)

In the special case when $n = 4$ and the pair of vertices guaranteed by Lemma 2.2 have curvature sum exactly 2π, the reduction does not apply, and the base case is a tetrahedron. The reason the reduction does not apply to this case is that Lemma 3.1 fails: p' would have to be on the bisector "at infinity." Although the reduction fails, there is a sense in which it can be carried out nevertheless, and we proceed in this section to demonstrate this to facilitate establishing the bases of the induction proofs.

Lemma 6.1 *An unbounded hexagon that results from applying the reduction to S_x for $n = 4$ with $\alpha_i + \alpha_{i+1} = 2\pi$, is an unfolding of a doubly-covered unbounded triangle, one with one bounded edge and two parallel unbounded edges.*

□

With this lemma available we may use $n = 3$ as the only base of the induction proofs, with the understanding that the doubly-covered triangle may be unbounded in the sense above.

7 Reduction Geometry

In this section we establish a crucial geometric lemma concerning the relative angles of edges in R' and R. This relationship derives ultimately from the fact that the curvature α' at p' is the sum of the curvatures α_i and α_{i+1}.

Lemma 7.1 (Reduction angles) *In the reduction $S_x \Rightarrow S'_x$, edge $x_{i-1}p'$ of S'_x is "exterior" to edge $x_{i-1}p_i$ of S_x, and edge $x_{i+1}p'$ is "exterior" to edge $x_{i+1}p_{i+1}$, in the sense that*

$$\angle p' x_{i-1} v \geq \angle p_i x_{i-1} v$$

$$\angle v x_{i+1} p' \geq \angle v x_{i+1} p_{i+1}$$

□

See Fig. 2: the dashed line bounding R' is exterior to R in the vicinity of $x_{i\pm1}$.

8 Sectors

Examination of Fig. 2 shows that in the $S'_x \Rightarrow S_x$ transition, R may extend beyond R', which presents a fundamental difficulty for a proof of nonoverlap of S_x from the nonoverlap of S'_x: nonoverlap of S'_x does not suffice – we need something stronger. The key "something stronger" is provided by a structural geometric constraint on the shape of the star unfolding, which we phrase in terms of circle sectors that lie just outside ∂S_x.

8.1 Definition of Sectors

We now define a region of the plane associated with each corner of a layout of S_x. The definition does not assume that S_x does not overlap, as it only depends on the positions of x_{i-1}, p_i, and x_i in the layout.

Define the *sector* s_i associated with p_i as the closed sector of the disk centered on p_i bounded by the radii $p_i x_{i-1}$ and $p_i x_i$, and exterior to S_x near p_i. The sectors for the unfolding of the pyramid shown in Fig. 4 are depicted in Fig. 6. We will see that the sector interiors are pairwise disjoint and exterior to S_x.

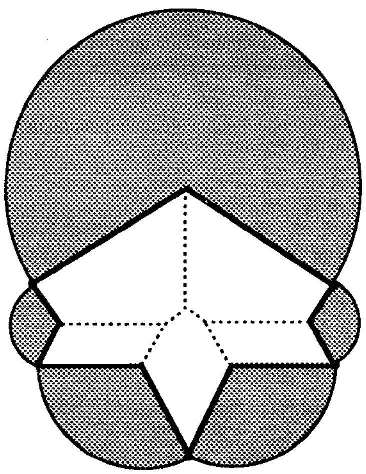

Figure 6: Sectors for the pyramid unfolding.

8.2 Sectors Nested

The key property of sectors is that the reduction implies a "nesting" of sectors in a certain sense, as illustrated in Fig. 7. We will see in the next section that this nesting implies that the sector interiors are pairwise disjoint and lie outside S_x. In preparation, we show that adjacent sectors are disjoint:

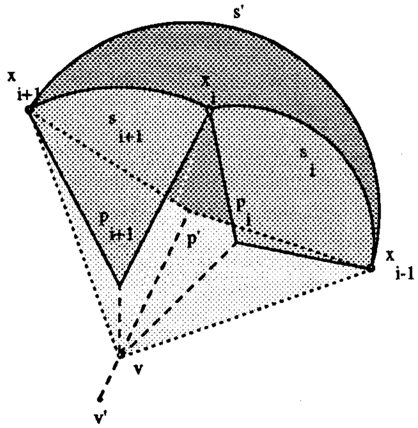

Figure 7: Nesting of sectors.

Lemma 8.1 *The interiors of adjacent sectors are disjoint.*

□

Lemma 8.2 (Sector nesting) *In the $S'_x \Rightarrow S_x$ transition, $R \cup s_i \cup s_{i+1} \subset R' \cup s'$.*

Proof: Recall that R is the hexagon $(v, x_{i-1}, p_i, x_i, p_{i+1}, x_{i+1})$ and R' is the quadrilateral $(v, x_{i-1}, p', x_{i+1})$ (see Fig. 7). Since R and R' have identical "inner" boundaries $x_{i-1}v \cup vx_i$, we only need to show that the "outer" boundary of $s_i \cup s_{i+1}$ falls inside the outer boundary of s'. This follows from the reduction angles lemma, Lemma 7.1. As $\angle v x_{i-1} p' \geq \angle v x_{i-1} p_i$, the normal to $x_{i-1}p'$, which is tangent to s', falls outside the normal to $x_{i-1}p_i$, which is tangent to s_i. The same is true at x_{i+1}. Thus the boundary arc of s_i incident to x_{i-1}, and the boundary arc of s_{i+1} incident to x_{i+1}, both fall inside s' in the vicinity of x_{i-1} and x_{i+1}, respectively. Both of these arcs end at x_i. It therefore only remains to show that x_i falls inside the outer boundary of s'.

Recall that x_{i-1}, x_i, and x_{i+1} all fall on a circle C centered on v (by the definition of the reduction). Because p' necessarily falls on the ray bisecting $\angle x_{i-1} v x_{i+1}$, C is inside the s' arc between x_{i-1} and x_{i+1}. Therefore x_i falls inside the s' arc. □

9 Nonoverlap

Let $Q_x = S_x \cup (\cup_j s_j)$ be the "complex" consisting of the star unfolding with the sectors glued in at their shared edges.

Theorem 9.1 (Nonoverlap) *The star unfolding augmented by the sectors, Q_x, does not overlap: S_x does not overlap with itself, the sectors do not overlap each other, and the sectors do not overlap with S_x.*

Proof: The proof is by induction.

Basis. As discussed in Section 6, the basis is a doubly-covered triangle, $n = 3$, although we must consider both bounded and unbounded triangles. We first discuss bounded triangles. Clearly S_x itself does not overlap in the bounded case, for it is the union of three peels glued together at the single ridge vertex. Each sector is clearly exterior to S_x. And every pair of the three sectors are adjacent to one another, so Lemma 8.1 shows that the sectors do not overlap one another. See Fig. 8.

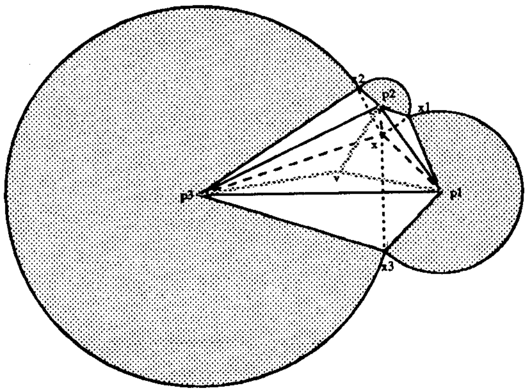

Figure 8: Sectors in the base case.

The proof for unbounded triangles is omitted. This completes the proof of nonoverlap in the unbounded case.

General Step. Assume $Q' = S'_x \cup (\cup_j s_j)$ does not overlap by induction. This means, in particular, that $R' \cup s'$, which is just a subset of Q', does not overlap with $Q' - (R' \cup s')$. But now by sector nesting (Lemma 8.2), $R \cup s_i \cup s_{i+1} \subset R' \cup s'$, so none of the changes made in the $S'_x \Rightarrow S_x$ transition cause overlap with $Q' - (R' \cup s')$. And clearly the portion added, $R \cup s_i \cup s_{i+1}$, does not overlap itself: R does not overlap s_i or s_{i+1} by construction, and the sectors are adjacent so Lemma 8.1 applies. Therefore

$$Q_x = [Q' - (R' \cup s')] \cup (R \cup s_i \cup s_{i+1})$$

does not overlap. $\square$

In particular, we have shown that S_x is a simple polygon.

10 The Voronoi Property

We prove in this section that the ridge tree is a subset of the Voronoi diagram of the source images. Recall that X is the set of source images in the unfolding. Let $\mathcal{V}(X)$ be the Voronoi diagram of X, viewed as a set of points in a layout of S_x in the plane. We prove that $T_x = \mathcal{V}(X) \cap S_x$. We will establish this by showing that a certain collection of "Voronoi disks" are empty of source images. Let D_y be the open disk centered on a point $y \in S_x$ with radius equal to the shortest path distance from x to y. We call D_y a *Voronoi disk*. The proof has the following outline:

1. Q_x (S_x augmented by the sectors) *contains the union* of the Voronoi disks D_y for all ridge points $y \in T_x$.
2. This containment implies that the Voronoi disks of all ridge points are *empty of source images.*
3. This implies that the Voronoi disk D_y of *any point* $y \in S_x$ is empty of source images. Moreover, among points in S_x, only ridge points have more than one source image on the boundary of their Voronoi disk.
4. The emptiness of the disks in turn implies the Voronoi property.

Steps (2)–(4) of the proof are easy, and we dispense with them prior to launching into the more difficult step (1).

(2) Suppose Q_x contains the Voronoi disks for all ridge points. The source images lie on the boundary of S_x, and the exterior arc bounding sector s_j begins and terminates at consecutive source images. As Q_x does not self-overlap (Theorem 9.1), the sources are on the boundary of Q_x. The emptiness of the disks follows immediately, as they are all open and contained in Q_x.

(3) Assume that the Voronoi disk of every ridge point is free of source images. Let $y \in S_x - T_x$. Suppose that y lies in the peel of x_j. Since peels are convex, by extending the shortest path $\pi(x, y)$ past y we obtain a point $z \in T_x$ with the property that all of $\pi(x, z)$ lies in the same peel. By assumption, D_z is free of source images and, by construction, x_j lies on the boundary ∂D_z of D_z. By definition of a Voronoi disk, D_y has radius $|yx_j|$ and thus lies inside D_z; moreover $\partial D_z \cap \partial D_y = \{x_j\}$. So D_y

is empty and its boundary contains exactly one source point, as claimed.

(4) Suppose now that the Voronoi disk for each point of S_x is empty of source images and no point of S_x outside T_x has more than one source image on the boundary of its Voronoi disk. This immediately implies that $T_x = \mathcal{V}(X) \cap S_x$, as $\mathcal{V}(X)$ is by definition the collection of points y in the plane for which the largest open disk centered at y and free of points of X touches two or more points of X.

The essence of the Voronoi property then reduces to (1) above, which we prove via induction based on the reduction used in the nonoverlap proof.

Lemma 10.1 *Q_x, the star unfolding augmented by the sectors, includes the union of all Voronoi disks for ridge points:*

$$\bigcup_{y \in T_x} D_y \subset Q_x.$$

□

Finally we may claim the second main result of this paper:

Theorem 10.2 (Voronoi property) *The ridge tree is the portion of the Voronoi diagram of the source images that lies inside the star unfolding: $T_x = \mathcal{V}(X) \cap S_x$.* □

11 Smooth Convex Surfaces

There is every reason to expect that our main theorems hold true for arbitrary convex surfaces as well as for polytopes. This leads us to make three conjectures for arbitrary convex surfaces:

1. The cut locus "develops" ("unfolds") in the plane without self-intersection. That the ridge tree unfolds without self-intersection is a consequence of nonoverlap, Theorem 9.1.

2. The star unfolding of the surface is a simple closed region of the plane, whose boundary is the locus of all source images. This is the generalization of Theorem 9.1, but we need to define what the star unfolding is in this context.

   First, develop the cut locus. Second, from each point y of the cut locus, draw segments in the plane corresponding to all the shortest paths from the source x that are incident to y. Draw each segment to have the length of the corresponding shortest path, and to make the same angle at the point y with the cut locus, as it does on the surface of $\mathcal{P}$. The star unfolding is this particular layout of all the shortest paths from x on $\mathcal{P}$.

3. The developed cut locus is the medial axis of the locus of the source images. The "medial" or "symmetric" axis of a Jordan curve is the locus of centers of interior disks that meet the curve in more than one point. This is the analog of the Voronoi property, Theorem 10.2.

12 Algorithmic Consequences

The primary consequence of our results is that it is now an easy matter to construct the ridge tree, formerly an object of formidable conceptual complexity: find shortest paths to all corners, build the star unfolding in the plane, and compute the conventional Voronoi diagram of the set of source images.[6] In particular, our results now justify Chen and Han's simple and efficient algorithm for single-source shortest path queries [CH90].

Second, in [AAOS91], an algorithm is presented for computing the exact set of edge sequences in $O(n^7 \log n)$ time. An edge sequence is a list of edges crossed by a shortest path; they are used for finding shortest paths amidst polyhedra [SS86]. A major factor in the algorithm's time complexity is the number of combinatorial changes the ridge tree may undergo as the source moves along a straight line without crossing a ridge of any corner. The only bound proved in [AAOS91] was $O(n^4)$. But knowing by Theorem 10.2 that the ridge tree is actually a subgraph of a Voronoi diagram, we may obtain an $O(n^3)$ bound on the number of changes using lower-envelope theory. This observation simplifies the algorithm and its analysis, but leaves its complexity at $O(n^7 \log n)$.

Third, the $O(n^{10})$ algorithm of [AAOS90] for computing the "geodesic diameter" of a polytope (the maximum possible separation between two points on its surface) may be improved by our results in two ways. At the

[6] This is how Fig. 1 was produced.

center of $O(n^9)$ iterations in that algorithm is a linear-time calculation to disambiguate possible overlap of the star unfolding, and an $O(n)$ visibility calculation. The first is obviated by our nonoverlap theorem (Theorem 9.1) and the second by the Voronoi property (Theorem 10.2). The result is an $O(n^9 \log n)$ algorithm for the diameter.

These algorithmic consequences will be developed in [AAOS91].

12.1 Acknowledgements

We thank Pankaj K. Agarwal and Catherine Schevon, our coauthors on [AAOS90] and [AAOS91], whose ideas have contributed significantly to this paper. The second author also thanks Robert Currier, Vladimir Oliker, and Andrejs Treibergs for pointers to the differential geometry literature.

References

[AO91] B. Aronov, and J. O'Rourke. Nonoverlap of the star unfolding. Technical report 002, Smith College, March 5, 1991.

[AAOS90] P. K. Agarwal, B. Aronov, J. O'Rourke, and C. Schevon. Star unfolding of a polytope with applications. In J. R. Gilbert and R. Karlsson, editors, *Proc. of 2nd Scandanavian Workshop on Algorithm Theory*, pages 251–263. Springer-Verlag, July 1990. Lecture Notes in Computer Science, Vol. 447.

[AAOS91] P. K. Agarwal, B. Aronov, J. O'Rourke, and C. Schevon. The star unfolding of a polytope. Technical report, Smith College, 1991. Full version of [AAOS90a]; currently under revision.

[Ale55] A. D. Aleksandrov. *Die Innere Geometrie der Konvexen Flächen.* Akademie-Verlag, Berlin, 1955. Math. Lehrbucher und Monographien.

[Ale58] A. D. Aleksandrov. *Konvexe Polyeder.* Akademie-Verlag, Berlin, 1958. Math. Lehrbucher und Monographien.

[Bus58] H. Buseman. *Convex Surfaces.* Interscience Publishers, New York, NY, 1958.

[CH90] J. Chen and Y. Han. Shortest paths on a polyhedron. In *Proc. of 6th ACM Symposium on Computational Geometry*, pages 360–369, 1990.

[Kob67] S. Kobayashi. *On conjugate and cut loci*, pages 96–122. Mathematical Association of America, 1967. S. S. Chern, Ed.

[Pog73] A. V. Pogorelov. *Extrinsic Geometry of Convex Surfaces.* American Mathematical Society, Providence, RI, 1973. Translations of Mathematical Monographs Vol. 35.

[SS86] M. Sharir and A. Schorr. On shortest paths in polyhedral spaces. *SIAM J. Comput*, 15:193–215, 1986.